Original Article

Stable COX17 Downregulation Leads to Alterations in Mitochondrial Ultrastructure, Decreased Copper Content and Impaired Cytochrome *c* Oxidase Biogenesis in HEK293 Cells

(Cox17 protein / copper chaperone / cytochrome *c* oxidase assembly / mitochondrial ultrastructure)

M. VANIŠOVÁ, D. BURSKÁ, J. KŘÍŽOVÁ, T. DAŇHELOVSKÁ, Ž. DOSOUDILOVÁ, J. ZEMAN, L. STIBŮREK, H. HANSÍKOVÁ

Laboratory for Study of Mitochondrial Disorders, Department of Paediatrics and Adolescent Medicine, First Faculty of Medicine, Charles University and General University Hospital in Prague, Czech Republic

Abstract. Cox17 is an assembly factor that participates in early cytochrome *c* oxidase (COX, CcO) assembly stages. Cox17 shuttles copper ions from the cytosol to the mitochondria and, together with Sco1 and Sco2, provides copper ions to the Cox1 and Cox2 mitochondrially encoded subunits. In *Saccharomyces cerevisiae*, Cox17 also modulates mitochondrial membrane architecture due to the interaction of Cox17 with proteins of the MICOS complex (mitochondrial contact site and cristae organizing system). There is currently no data regarding the impact of long-term Cox17 deficiency in human cells. Here, we present construction and characterization of three stable COX17 shRNA-downregulated HEK293 cell lines that have less than 10 % of the residual Cox17 protein level. Cox17-depleted cell lines exhibited decreased intramitochondrial copper content, decreased CcO subunit levels (Cox1, Cox4 and Cox5a) and accumulation of CcO subcomplexes. Similarly to yeast cells, mitochondria in Cox17-downregulated HEK293 cell lines exhibited ultrastructural changes including cristae reduction and mitochondrial swelling. Characterization of the molecular pathogenesis of long-term Cox17 deficiency complements our knowledge of the mitochondrial copper metabolism and assembly of cytochrome *c* oxidase in human cells.

Corresponding author: Hana Hansíková, Department of Paediatrics and Adolescent Medicine, First Faculty of Medicine, Charles University and General University Hospital in Prague, Ke Karlovu 2, 128 08 Prague 2, Czech Republic. Phone: (+420) 224 967 748; e-mail: hana.hansikova@lf1.cuni.cz

Abbreviations: AAS – atomic absorption spectroscopy, ATP – adenosine triphosphate, COX, CcO – cytochrome *c* oxidase, Cox1, Cox2, Cox4, Cox5a – subunits of cytochrome *c* oxidase, Cox17A, Cox17B, Cox17C – cell lines stably silenced for Cox17 protein, CuA, CuB – copper centres in cytochrome *c* oxidase active site, DDM – n-dodecyl β-d-maltoside, DMEM – Dulbecco's modified Eagle's medium, EDTA – ethylenediaminetetraacetic acid, FBS – foetal bovine serum, GFP – green fluorescent protein, HEK293 – human embryonic kidney cells, IMS – intermembrane space, KD – knockdown, MICOS – mitochondrial contact site and cristae organizing system, mtDNA – mitochondrial DNA, nDNA – nuclear DNA, NS – non-silencing cells, OXPHOS – oxidative phosphorylation system, PBS – phosphate-buffered saline, PIC – protease inhibitor cocktail, PMSF – phenylmethylsulphonyl fluoride, RNAi – RNA interference, Sco1, Sco2, Cox11, Cox17, Cox19, CoA6, Cox23 – copper chaperones, shRNA – short hairpin RNA, TEM – transmission electron microscopy, WT – wild type.

Introduction

Mitochondrial cytochrome *c* oxidase (COX, complex IV, CcO) is one of the five complexes of the oxidative phosphorylation system (OXPHOS) in which more than 90 % of ATP molecules are produced to supply the cellular energy demand. CcO, together with OXPHOS complexes I, II and III, generate a proton gradient across the inner mitochondrial membrane through oxidation of NADH and FADH$_2$ cofactors, which is then used by ATP synthase to generate ATP. Mitochondria fulfil many other important functions, including amino acid metabolism, purine synthesis, serving as a calcium repository and restoring the cellular copper pool (Baker et al., 2017; Bravo-Sagua et al., 2017; Ducker and Rabinowitz 2017; Chan et al., 2018).

Mammalian CcO is a hetero-oligomeric complex, which, for a long time, has been considered to be composed of 13 structural subunits (Kadenbach et al., 1983). Outcomes of some recent studies (Balsa et al., 2012; Pitceathly et al., 2013), although still debated (Kadenbach, 2017; Pitceathly and Taanman, 2018), call for reconsideration of CI structural subunit NDUFA4 to be the 14th CcO structural subunit COXFA4 instead. Subunits Cox1, Cox2 and Cox3, which constitute the catalytic centre of CcO, are encoded by mitochondrial DNA

(mtDNA) and synthesized in mitochondria. Cox1 and Cox2 contain redox-active copper cofactors (CuA and CuB) and two haem centres (haem a and haem a_3). They are involved in electron transport to the terminal acceptor oxygen and are essential for the catalytic function of CcO (Stiburek et al., 2006). Both Cox1 and Cox2 are incorporated during the early stages of CcO assembly along with Cox3. The remaining 10 structural subunits, encoded by nuclear DNA (nDNA), are posttranslationally transported to the mitochondria. Several of these subunits are expressed as tissue-specific isoforms and are required to protect the catalytic centre and stabilize CcO within the membrane (Beauvoit et al., 1999, Balsa et al., 2012). Additionally, more than 30 auxiliary factors, called assembly proteins, participate in the CcO assembly process (Barrientos et al., 2002).

One of these assembly factors – Cox17 – is a specific copper donor to both Sco1 and Cox11 assembly factors in the mitochondrial intermembrane space (IMS). In cooperation with other factors such as Sco2, Cox19, CoA6 and Cox23, Cox17 functions to deliver copper ions to the active sites of the CcO Cox1 and Cox2 subunits (Carr and Winge 2003; Palumaa et al., 2004; Pacheu-Grau et al., 2015). It was recently reported that mitochondrial phosphate carrier SLC25A3 can also serve as a copper chaperone in CcO biogenesis (Boulet et al., 2018).

It is supposed that Cox17 shuttles copper ions from the cytosol to the mitochondria to incorporate them into CcO (Glerum et al., 1996), but some studies with yeast suggest that Cox17 functions only in the mitochondrial IMS (Maxfield et al., 2004). Cox17 can bind four copper ions via evolutionarily conserved metal-binding cysteine residues and is transferred into the mitochondrial intermembrane space via the Mia40/Erv1 pathway (Palumaa et al., 2004).

In 2015, it was discovered that Cox17 is involved in regulating the mitochondrial inner membrane integrity via its interaction with Mic60 of the MICOS complex (mitochondrial contact site and cristae organizing system) (Chojnacka et al., 2015).

In the yeast, Cox17 deficiency leads to the functional impairment of CcO, respiratory chain deficiency and impaired growth on non-fermentable substrates (Glerum et al., 1996). In HeLa cells, transient Cox17 silencing affected supercomplex organization of the OXPHOS complexes. This study supports the role of Cox17 as a copper shuttle between the cytosol and mitochondrial intermembrane space, where 80 % of the Cox17 cellular pool is localized (Oswald et al., 2009). Cox17 knockout mice showed embryonic lethality (Takahashi et al., 2002). As yet, no patients with mutations of the *Cox17* gene have been described.

Defects in copper transport to CcO (Sco1, Sco2) have been previously described in humans (Stiburek et al., 2009). These defects typically have a fatal impact on mitochondrial function and are characterized by a serious clinical phenotype with an unfavourable prognosis.

In the present study, we characterized the impact of the long-term (stable) depletion of Cox17 on the mitochondrial structure and function of HEK293 cells.

Material and Methods

Cell culture

Human embryonic kidney cells (HEK293) (American Type Culture Collection, Rockville, MD) were used for stable transfection and cultivation. The cells were grown at 37 °C in a humidified 5% (v/v) CO$_2$ atmosphere in Dulbecco's modified Eagle's medium (DMEM, Sigma-Aldrich – Merck, Darmstadt, Germany) supplemented with 10% (v/v) foetal bovine serum (FBS, Thermo Fisher Scientific, Waltham, MA).

shRNA constructs and cell transfection

To produce RNA interference (RNAi) in HEK293 cells, we used the pGIPZ plasmid (Open Biosystems, Dharmacon, Lafayette, CO), in which short hairpin RNA (shRNA) is expressed as human microRNA-30 (miR-30) primary transcript. In addition to generating shRNA, the primary transcript leads to the production of TurboGFP and puromycin N-acetyl transferase, thus allowing visual marking and selection of shRNA-expressing cells. Three predesigned pGIPZ constructs for specific silencing of human COX17 (V3LHS_336599, V3LHS_405108 and V3LHS_336598) and a non-silencing control (NS) were purchased from Open Biosystems (Dharmacon, Lafayette, CO).

Subconfluent HEK293 cells were transfected by electroporation using Amaxa™ Nucleofection™ Technology (Lonza, Walkersville, MD) with a cell-specific kit according to the manufacturer's instructions. Transfected cells were selected using puromycin (Sigma-Aldrich-Merck) at a concentration of 5 μg/ml over a period of three weeks. The residual levels of Cox17 protein in the stable knockdown cell lines were quantified by SDS-PAGE immunoblot of whole cell lysates using Cox17-specific polyclonal antibodies (ab139375 and ab115309, Abcam, Cambridge, United Kingdom). The cell line transfected with the non-silencing shRNA construct (NS) and original HEK293 cells (WT) were used as controls.

Protein analysis

Total cellular protein was prepared by extraction in RIPA buffer [50 mM Tris/HCl – pH 7.4, 150 mM NaCl, 1 mM PMSF, 1 mM EDTA, 1% Triton X-100 and 0.1% (w/v) SDS] with 1% (v/v) protease inhibitor cocktail (PIC, Sigma-Aldrich-Merck) on ice for 20 min, followed by centrifugation at $51,000 \times g$ for 25 min at 4 °C. The protein concentration was determined by the Lowry method using BSA as a standard (Lowry et al., 1951). Samples were dissolved in SDS-PAGE sample buffer [50 mM Tris/HCl – pH 6.8, 12% (v/v) glycerol, 4% (w/v) SDS, 2% (v/v) 2-mercaptoethanol, 0.01% (w/v) bromophenol blue] by incubation at 37 °C for 30 min. Samples of 5–20 μg protein in each lane were resolved

by tricine-SDS-PAGE in 12% polyacrylamide minigels using the MiniProtean®3 System (Bio-Rad Laboratories, Hercules, CA). Proteins were electrotransferred from gels onto PVDF membranes (Immobilon-P, Millipore-Merck, Darmstadt, Germany) using semidry Western blot transfer, as previously described (Stiburek et al., 2005). Immunodetection was performed with the following antibodies: Cell Signaling Technology (Danvers, MA) α-tubulin – α-Tubulin (11H10) rabbit mAb, 2125S, 1 : 2000 (Abcam) Cox17 – anti-COX17 – N-terminal, ab139375, 1 : 2000; Cox1 – anti-MTCO1 [1D6E1A8], ab14705, 1 : 5000; Cox2 – anti-MTCO2 [12C4F12], ab110258, 1 : 2000 Cox4 – anti-COX IV [20E8C12], ab14744, 1 : 2000; Cox5a – anti-COX5A [6E9B12D5], ab110262, 1 : 2000; Sco1 – anti-SCO1, ab88658, 1 : 5000; Sco2 – anti-SCO2, ab169042, 1 : 10,000. All samples were normalized to the amount of α-tubulin and total protein loading.

Blue native polyacrylamide gel electrophoresis (BN-PAGE) (Schagger and von Jagow, 1991) was used to separate mitochondrial membrane protein complexes in polyacrylamide 6–15% (w/v) gradient gels using a Mini-Protean®3 system (Bio-Rad Laboratories). Isolated mitochondria were solubilized with n-dodecyl β-d-maltoside (DDM; Sigma-Aldrich - Merck), with a final DDM/protein ratio of 4.8 g/g in a buffer containing 1.5 M aminocaproic acid, 2 mM EDTA and 50 mM 2-bis(2-hydroxyethyl)amino-2-(hydroxymethyl)-1,3-propanediol – pH 7.0 at 4 °C for 20 min. The samples were then centrifuged for 20 min at $51,000 \times g$ and 4 °C. Serva Blue G dye (Serva, Heidelberg, Germany) was added to the collected supernatant at a concentration of 0.1 g/g of detergent. A 20 μg aliquot of protein was loaded in each lane. The electrophoresis was performed at 30 V, 4 °C for 30 min, then at 40 V, 4 °C for 2 h and then overnight at 25 V, 4 °C.

For the second dimension of the two-dimensional BN/SDS-PAGE, strips of the first-dimension gels were incubated for 40 min in 1% (v/v) 2-mercaptoethanol and 1% (w/v) SDS and washed for 30 min in water. The denatured proteins were then resolved in the second dimension with a 12% polyacrylamide SDS gel. The OXPHOS complex subunits were transferred to PVDF membranes and probed with the following antibodies: Cox1 – anti-MTCO1 [1D6E1A8], Abcam ab14705, 1 : 5000; anti-SDHA (MitoSciences, Eugene, OR, MS203, 1 : 7000).

All immunoreactive material was visualized by chemiluminescence using horseradish peroxidase-conjugated secondary anti-mouse (A0545) or anti-rabbit (A8924) antibodies (Sigma-Aldrich-Merck) and SuperSignal West Femto Maximum Sensitivity Substrate (Thermo Scientific, Rockford, IL). Signal acquisition was performed using a G: Box SynGene imaging system (Syngene, Cambridge, United Kingdom).

Isolation of mitochondria

Mitochondria were isolated from frozen (–80 °C) pellets of harvested KD and control HEK293 cells by homogenization at 4 °C with a glass/glass Dounce homogenizer in isotonic medium [250 mM sucrose, 10 mM Tris, 1 mM EDTA, pH 7.4] (STE buffer) with 1% (v/v) protease inhibitor cocktail (PIC, Sigma-Aldrich-Merck). The homogenate was centrifuged for 15 min at $600 \times g$, 4 °C. The supernatant was then centrifuged for 25 min at $10,000 \times g$, 4 °C in order to pellet the mitochondria. The pellet was washed with STE buffer and re-isolated by centrifugation as described above. The mitochondria were then resuspended in STE buffer (2.5 volume of the pellet), divided into aliquots and stored at –80 °C for subsequent analyses.

Transmission electron microscopy (TEM)

HEK293 cells were cultivated to 90% confluence and fixed in 1× phosphate-buffered saline (PBS, BioWhittaker, Lonza, Walkersville, MD) containing 2% (w/v) potassium permanganate for 15 min at room temperature (RT). After fixation, cells were dehydrated by ethanol series (for 10 min in 50%, 70% and 90% ethanol, for 30 min in 100% ethanol). Samples were incubated in propylene oxide (2 x 15 min) and embedded in Durcupan Epon (Durcupan Epon : propylene oxide 1 : 1 for 2 h, Durcupan Epon : propylene oxide 1 : 3 overnight). Polymerized blocks were sectioned by an Ultracut Reichert microtome. Slices of thickness 600-900A were stained with lead citrate and uranyl acetate (Brantova et al., 2006). Images were acquired with a JEOL JEM 1400 (Plus) transmission electron microscope (JEOL, Peabody, MA).

Epifluorescence microscopy

Cox17 KD and control HEK293 cells were grown on cover glasses. The mitochondria were stained using vital probe 10 nM MitoTracker Red CMX Ros (Molecular Probes, Eugene, OR) for 15 min at 37 °C. Next, the cells were washed with 1× PBS (PBS, BioWhittaker, Lonza, Walkersville, MD) and the mitochondrial network was detected by a Nikon Diaphot 200 inverted microscope (Nikon, Tokyo, Japan). The images were acquired with an Olympus DP50 CCD camera and Viewfinder Lite 1.0 software (Pixera, Santa Clara, CA).

Atomic absorption spectroscopy

To determine the total copper content in the cells and isolated mitochondria after sample mineralization we used inductively coupled plasma mass spectrometry (ICP-MS). The sample was weighed into high-pressure Teflon (TFM) vessels and digested with a mixture of HNO_3 and H_2O_2 in microwave oven Milestone Ethos 1 (Milestone, Italy). After mineralization and evaporation of acids, the mineralizate was diluted with deionized water to a total volume of 10 ml. The determination of total copper concentration in mineralized samples was performed using an Elan DRC-e spectrometer (Perkin-Elmer SCIEX, Norwalk, CT) equipped with a concentric glass nebulizer and quartz cyclonic spray chamber.

The isotope ^{63}Cu was used for quantification and germanium ^{74}Ge was used as an internal standard. The external calibration curve for copper was in the range of

0–50 µg copper/l, the concentration of internal standard Ge was 10 µg/l. Blank samples were processed with the tested samples. The quality control was performed using samples of reference material INCT MPH 2 (INCT, Warsaw, Poland) with a copper concentration of 7.7 mg/kg sample. The recovery of the reference material was 98.2–99.6 %.

Results

Cox17 protein levels were successfully knocked down by shRNA expression in HEK293 cells

The HEK293 cell lines Cox17A, Cox17B and Cox17C were successfully stably silenced for Cox17 protein expression. After 21 days of cultivation, 100 % of the transfected cells were green fluorescent protein (GFP) positive. The reduction in Cox17 protein levels in the silenced cells was identified by SDS-PAGE immunoblot of whole-cell lysates. All three Cox17-silenced lines (Cox17A, Cox17B and Cox17C) showed a significant decline in the Cox17 protein level to less than 10 % of the control values. The immunoblot signal of the Cox17 protein in the Cox17C-downregulated cell line was almost undetectable (Fig. 1A).

The mitochondrial copper level was decreased in Cox17-silenced cells

AAS was used to determine the amount of copper ions in Cox17-downregulated and control cells. Analysis was performed in whole-cell samples and in isolated mitochondrial fractions of Cox17-depleted and control cell lines. The isolated mitochondria samples showed decreased levels of copper ions in all Cox17-depleted cell lines compared to the mitochondrial fraction from controls. The copper content in the mitochondria from the Cox17-silenced cell lines was between 70 % and 80 % of the control values (Fig. 2). Identical analysis carried out in whole-cell samples failed to show significant differences between the control and Cox17-downregulated cell lines (data not shown).

Cox17-silenced cells showed impaired mitochondrial ultrastructure

In all three cell lines, the mitochondrial ultrastructure of the Cox17-downregulated cells showed moderate disturbances including mitochondrial swelling and cristae disorganization. While swollen mitochondria were frequently observed in the Cox17A, Cox17B and Cox17C
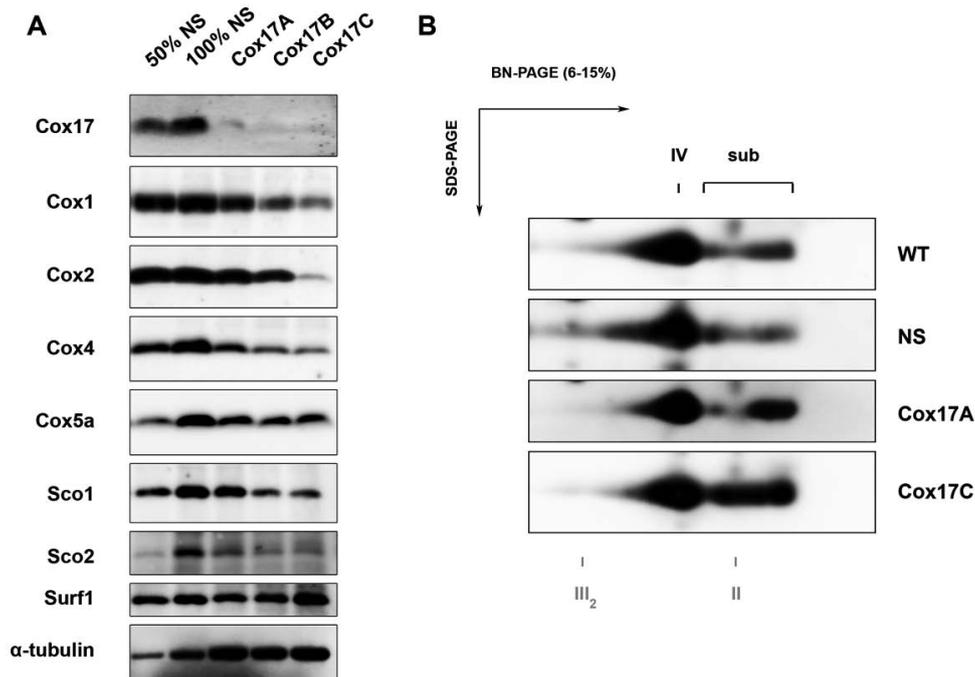
Fig. 1. Effect of Cox17 depletion on the structure and assembly of complex IV (CcO)
(A) Immunoblot analysis of control (NS) and Cox17-depleted (Cox17A-C) samples under denaturing conditions. Equal amounts (20 µg) of total cell lysates were resolved by SDS-PAGE and subjected to immunoblot analysis with antibodies raised against selected assembly factors (Cox17, Sco1, Sco2, Surf1) and structural subunits (Cox1, 2, 4, 5a) of CcO. The level of α-tubulin was monitored as a loading control. **(B)** Immunoblot analysis of control (NS, WT) and Cox17-depleted samples (Cox17A,C) under native conditions. Equal amounts (20 µg) of mitochondrial protein prepared by solubilization using 1.1% DDM (4.8 g DDM/g protein) were resolved by 2D BN/SDS PAGE and subjected to immunoblot analysis. CcO holoenzyme (IV) and assembly intermediates (sub) were detected with antibody against the Cox1 subunit. The migration direction of the first (native) gradient (BN-PAGE 6-15 %) and the second (denaturing) (SDS-PAGE) dimension are indicated. The migration of respiratory chain complexes III (III_2) and II are marked (grey Roman numerals).
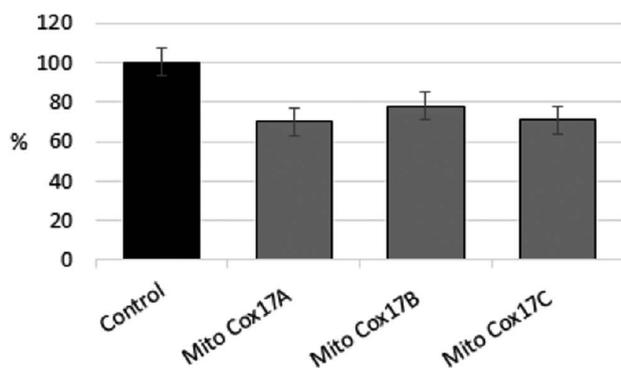
Fig. 2. Total copper content in mitochondria isolated from Cox17-silenced (Cox17A-C) and control (NS) HEK293 cells

Analysis was carried out by atomic absorption spectroscopy with the ICP-MS method. The control value represents 100 %.

lines, this phenotype was rarely detected in control cells. The most intensive mitochondrial swelling was found in the Cox17C line, corresponding with the lowest residual Cox17 level in these cells (Fig. 3).

Due to the changes in mitochondrial ultrastructure, we also visualized the mitochondrial network in cultivated cells using native fluorescent dye (MitoTracker
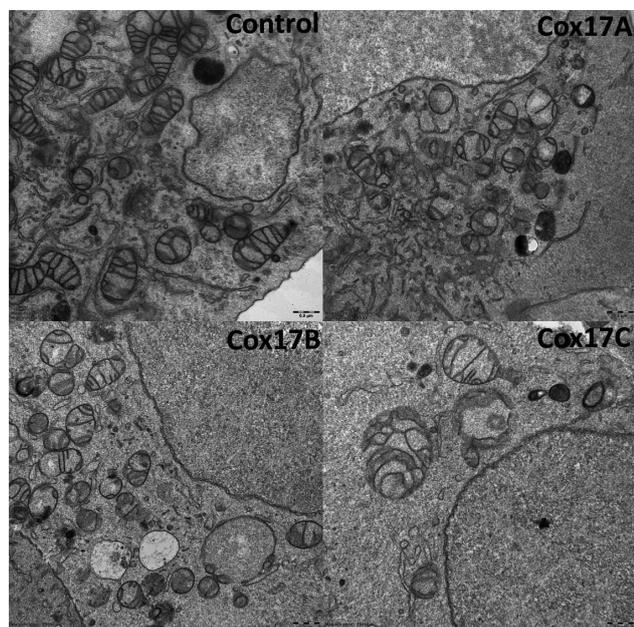
Fig. 3. Effects of Cox17 depletion on the mitochondrial ultrastructure in Cox17 knockdown HEK293 cell lines (Cox17A, B and C) in comparison with control (NS)

Mild mitochondrial swelling and cristae disorganization were detected in all Cox17-silenced cell lines in comparison with control lines. The most prominent alterations were observed in the Cox17C line. Selected images show representative examples. Original magnification: 25,000 ×, Jeol JEM1400+

Red CMX Ros, Molecular Probes, Eugene, OR). In contrast to the mitochondrial ultrastructure, the mitochondrial network did not show any significant changes in the Cox17-downregulated cell lines compared to the controls (data not shown).

Western blot analysis of complex IV showed diminished amounts of CcO subunits and accumulation of early CcO assembly intermediates

SDS-PAGE and immunoblot analyses showed marked decreases in all tested CcO subunits except for Cox2 in the Cox17A line, which corresponded to 85 % of the control value (Fig. 1A). In the Cox17B and Cox17C lines, Cox2 subunit levels were decreased to 57 % and 11 %, respectively. Cox1 subunit levels were decreased to 78 % in the Cox17A line, to 53 % in the Cox17B line and to 33 % in the Cox17C line. Cox4 subunit levels were decreased to less than 60 % of the control values in all silenced cell lines (Cox17A: 52 %, Cox17B: 33 %, Cox17C: 24 %). Cox5a subunit levels were decreased to 72 % in the Cox17A line, to 60 % in the Cox17B line and to 57 % in the Cox17C line compared to the controls. The almost complete absence of Cox17 protein was accompanied by a significant reduction of Sco1 and Sco2 proteins. Sco1 protein levels were reduced to 73 % in Cox17A, to 37 % in Cox17B and to 39 % in Cox17C cell lines. Sco2 protein levels were reduced to 75 % in Cox17A and to 65 % in both Cox17B and Cox17C cell lines.

2D BN/SDS-PAGE immunoblot analysis revealed increased accumulation of CcO assembly intermediates in all Cox17-silenced cell lines (Fig. 1B).

Discussion

Most of the current knowledge of the Cox17 protein function is based on yeast studies. Cox17 is a metallochaperone thought to traffic copper ions to mitochondrial CcO (Palumaa et al., 2004). In the yeast, Cox17 defects lead to CcO deficiency and growth impairment (Glerum et al., 1996). However, deletion of Cox17 in *Saccharomyces cerevisiae* does not affect the mitochondrial copper content (Cobine et al., 2004). The Cox17 protein is imported to the IMS via the MIA40/Erv1 pathway (Mesecke et al., 2005). In contrast to these studies, the Cox17 protein function in human cells is poorly understood. A mouse COX17 knockout model presented with embryonic lethality (Takahashi et al., 2002). In 2009, it was reported that transient Cox17 silencing in HeLa cells blocks CcO assembly (Oswald et al., 2009). No data about stable, long-term Cox17 deficiency are known, and no patient with a Cox17 mutation has yet been described. Mutations in Cox17 binding partners Sco1 and Sco2 are associated with mitochondrial impairment and hypertrophic cardiomyopathy (reviewed in Baker et al., 2017).

In our study, we analysed how the stable shRNA silencing of Cox17 expression affects mitochondrial struc-

ture and function in the HEK293 cell model. Three HEK293 cell lines stably silenced for Cox17 protein expression (Cox17A, Cox17B, Cox17C) were successfully generated and characterized. The amount of Cox17 protein was knocked down to less than 10 % of the control values in all three generated cell lines. The content of copper ion in the mitochondria of downregulated cells was reduced to 70–80 % of control values in all of the three silenced cell lines. We can speculate that the relatively high residual level of intramitochondrial copper in Cox17-downregulated cells could stem from the existence of alternative copper shuttle proteins with functions that are redundant to Cox17 (Baker et al., 2017). Another explanation might be that human Cox17 does not function in copper transport to mitochondria and operates functionally only in the mitochondrial IMS, where it transports copper to CcO active sites (with its binding partners), similarly to the situation observed in the yeast (Maxfield et al., 2004). In this scenario, the diminished copper content in Cox17-downregulated mitochondria could be caused by feedback signalling due to the decreased Cox17, Sco1 and Sco2 protein levels (Fig. 3). The signalling role of CcO assembly factors Sco1 and Sco2 in CcO deficiency has been previously described (Leary, 2010; Dodani et al., 2011).

In the yeast, besides its role as a CcO assembly factor, Cox17 transiently associates with MICOS complexes and regulates the inner mitochondrial membrane architecture and its phospholipid composition (Chojnacka et al., 2015). We analysed the mitochondrial structure of Cox17-downregulated cell lines by TEM. In Cox17A, Cox17B and (especially) Cox17C, the TEM analysis showed cristae disorganization and mitochondrial swelling, which is in agreement with the suggested role of Cox17 in controlling the inner mitochondrial membrane organization (Chojnacka et al., 2015).

Immunoblot analysis of the Cox17-silenced cell lines under denaturing conditions showed markedly reduced levels of selected CcO subunits (Cox1, Cox2, Cox4, Cox5a). Moreover, 2D blue-native/denaturing immunoblotting showed increased accumulation of several CcO assembly intermediates in the mitochondria of COX17-silenced cells. CcO contains three copper ions within two copper centres (CuA and CuB) of the Cox1 and Cox2 subunits, respectively. Failure to provide copper ions to Cox1 and Cox2 likely abrogates the assembly of these crucial core subunits into the CcO complex, leading to the appearance of early CcO assembly intermediates (Baker et al., 2017; Jett and Leary, 2018). These subassemblies lack the protection of nuclear-encoded CcO subunits, rendering them accessible to proteolysis by mitochondrial proteases and leading to stalled CcO holoenzyme assembly (Cesnekova et al., 2016). In addition to CcO subunits, the immunoblot analysis showed reduced amounts of both Sco1 and Sco2 metallochaperones in our Cox17-silenced cell lines. Indeed, the binding of copper ions, as well as the interaction with Cox17, is likely to stabilize Sco1 and Sco2 (Baker et al., 2017, Jett and Leary 2018). In addition to the Sco metal-

lochaperones, the immunoblot analysis revealed a moderate reduction of the Surf1 protein in our Cox17 cells. Whereas the yeast homologue of Surf1 is likely involved in the haemylation of the Cox1 subunit, mammalian Surf1 is probably involved in assembling Cox2 into the CcO complex (Hannappel et al., 2012; Quadalti et al., 2018). Hence, the markedly reduced Cox2 levels in our Cox17 cell lines might compromise the stability of Surf1 through the diminished formation of Surf1-Cox2 complexes.

In conclusion, our study has shown that Cox17 plays a direct role in CcO assembly/stability and that the loss of Cox17 function in HEK293 cells affects the level of intramitochondrial copper and impairs the morphogenesis of mitochondrial cristae. Further knowledge of the role of human Cox17 will help us to understand the underlying pathomechanisms of CcO assembly defects in humans.

References

Baker, Z. N., Cobine, P. A., Leary, S. C. (2017) The mitochondrion: a central architect of copper homeostasis. *Metallomics* **9**, 1501-1512.

Balsa, E., Marco, R., Perales-Clemente, E., Szklarczyk, R., Calvo, E., Landazuri, M. O., Enriquez, J. A. (2012) NDU-FA4 is a subunit of complex IV of the mammalian electron transport chain. *Cell Metab.* **16**, 378-386.

Barrientos, A., Barros, M. H., Valnot, I., Rotig, A., Rustin, P., Tzagoloff, A. (2002) Cytochrome oxidase in health and disease. *Gene* **286**, 53-63.

Beauvoit, B., Bunoust, O., Guerin, B., Rigoulet, M. (1999) ATP-regulation of cytochrome oxidase in yeast mitochondria: role of subunit VIa. *Eur. J. Biochem.* **263**, 118-127.

Boulet, A., Vest, K. E., Maynard, M. K., Gammon, M. G., Russell, A. C., Mathews, A. T., Cole, S. E., Zhu, X., Phillips, C. B., Kwong, J. Q., Dodani, S. C., Leary, S. C., Cobine, P. A. (2018) The mammalian phosphate carrier SLC25A3 is a mitochondrial copper transporter required for cytochrome c oxidase biogenesis. *J. Biol. Chem.* **293**, 1887-1896.

Brantova, O., Tesarova, M., Hansikova, H., Elleder, M., Zeman, J., Sladkova, J. (2006) Ultrastructural changes of mitochondria in the cultivated skin fibroblasts of patients with point mutations in mitochondrial DNA. *Ultrastruct. Pathol.* **30**, 239-245.

Bravo-Sagua, R., Parra, V., Lopez-Crisosto, C., Diaz, P., Quest, A. F., Lavandero, S. (2017) Calcium transport and signaling in mitochondria. *Compr. Physiol.* **7**, 623-634.

Carr, H. S., Winge, D. R. (2003) Assembly of cytochrome c oxidase within the mitochondrion. *Acc. Chem. Res* **36**, 309-316.

Cesnekova, J., Rodinova, M., Hansikova, H., Houstek, J., Zeman, J., Stiburek, L. (2016) The mammalian homologue of yeast Afg1 ATPase (lactation elevated 1) mediates degradation of nuclear-encoded complex IV subunits. *Biochem. J.* **473**, 797-804.

Cobine, P. A., Ojeda, L. D., Rigby, K. M., Winge, D. R. (2004) Yeast contain a non-proteinaceous pool of copper in the mitochondrial matrix. *J. Biol. Chem.* **279**, 14447-14455.

Dodani, S. C., Leary, S. C., Cobine, P. A., Winge, D. R., Chang, C. J. (2011) A targetable fluorescent sensor reveals that copper-deficient SCO1 and SCO2 patient cells prioritize mitochondrial copper homeostasis. *J. Am. Chem. Soc.* **133**, 8606-8616.

Ducker, G. S., Rabinowitz, J. D. (2017) One-carbon metabolism in health and disease. *Cell Metab.* **25**, 27-42.

Glerum, D. M., Shtanko, A., Tzagoloff, A. (1996) Characterization of COX17, a yeast gene involved in copper metabolism and assembly of cytochrome oxidase. *J. Biol. Chem.* **271**, 14504-14509.

Hannappel, A., Bundschuh, F. A., Ludwig, B. (2012) Role of Surf1 in heme recruitment for bacterial COX biogenesis. *Biochim. Biophys. Acta* **1817**, 928-937.

Chan, C. Y., Pedley, A. M., Kim, D., Xia, C., Zhuang, X., Benkovic, S. J. (2018) Microtubule-directed transport of purine metabolons drives their cytosolic transit to mitochondria. *Proc. Natl. Acad. Sci. USA* **115**, 13009-13014.

Chojnacka, M., Gornicka, A., Oeljeklaus, S., Warscheid, B., Chacinska, A. (2015) Cox17 protein is an auxiliary factor involved in the control of the mitochondrial contact site and cristae organizing system. *J. Biol. Chem.* **290**, 15304-15312.

Jett, K. A., Leary, S. C. (2018) Building the CuA site of cytochrome c oxidase: A complicated, redox-dependent process driven by a surprisingly large complement of accessory proteins. *J. Biol. Chem.* **293**, 4644-4652.

Kadenbach, B., Jarausch, J., Hartmann, R., Merle, P. (1983) Separation of mammalian cytochrome c oxidase into 13 polypeptides by a sodium dodecyl sulfate-gel electrophoretic procedure. *Anal. Biochem.* **129**, 517-521.

Kadenbach, B. (2017) Regulation of mammalian 13-subunit cytochrome c oxidase and binding of other proteins: role of NDUFA4. *Trends Endocrinol. Metab.* **28**, 761-770.

Leary, S. C. (2010) Redox regulation of SCO protein function: controlling copper at a mitochondrial crossroad. *Antioxid. Redox Signal.* **13**, 1403-1416.

Lowry, O. H., Rosebrough, N. J., Farr, A. L., Randall, R. J. (1951) Protein measurement with the Folin phenol reagent. *J. Biol. Chem.* **193**, 265-275.

Maxfield, A. B., Heaton, D. N., Winge, D. R. (2004) Cox17 is functional when tethered to the mitochondrial inner membrane. *J. Biol. Chem.* **279**, 5072-5080.

Mesecke, N., Terziyska, N., Kozany, C., Baumann, F., Neupert, W., Hell, K., Herrmann, J. M. (2005) A disulfide relay system in the intermembrane space of mitochondria that mediates protein import. *Cell* **121**, 1059-1069.

Oswald, C., Krause-Buchholz, U., Rodel, G. (2009) Knockdown of human COX17 affects assembly and supramolecular organization of cytochrome c oxidase. *J. Mol. Biol.* **389**, 470-479.

Pacheu-Grau, D., Bareth, B., Dudek, J., Juris, L., Vogtle, F. N., Wissel, M., Leary, S. C., Dennerlein, S., Rehling, P., Deckers, M. (2015) Cooperation between COA6 and SCO2 in COX2 maturation during cytochrome c oxidase assembly links two mitochondrial cardiomyopathies. *Cell Metab.* **21**, 823-833.

Palumaa, P., Kangur, L., Voronova, A., Sillard, R. (2004) Metal-binding mechanism of Cox17, a copper chaperone for cytochrome c oxidase. *Biochem J.* **382**, 307-314.

Pitceathly, R. D., Rahman, S., Wedatilake, Y., Polke, J. M., Cirak, S., Foley, A. R., Sailer, A., Hurles, M. E., Stalker, J., Hargreaves, I., Woodward, C. E., Sweeney, M. G., Muntoni, F., Houlden, H., Taanman, J. W., Hanna, M. G., Consortium, U. K. (2013) NDUFA4 mutations underlie dysfunction of a cytochrome c oxidase subunit linked to human neurological disease. *Cell Rep.* **3**, 1795-1805.

Pitceathly, R. D. S., Taanman, J. W. (2018) NDUFA4 (Renamed COXFA4) is a cytochrome-c oxidase subunit. *Trends Endocrinol. Metab.* **29**, 452-454.

Quadalti, C., Brunetti, D., Lagutina, I., Duchi, R., Perota, A., Lazzari, G., Cerutti, R., Di Meo, I., Johnson, M., Bottani, E., Crociara, P., Corona, C., Grifoni, S., Tiranti, V., Fernandez-Vizarra, E., Robinson, A. J., Viscomi, C., Casalone, C., Zeviani, M., Galli, C. (2018) SURF1 knockout cloned pigs: Early onset of a severe lethal phenotype. *Biochim. Biophys. Acta Mol. Basis Dis.* **1864**, 2131-2142.

Schagger, H., von Jagow, G. (1991) Blue native electrophoresis for isolation of membrane protein complexes in enzymatically active form. *Anal. Biochem.* **199**, 223-231.

Stiburek, L., Vesela, K., Hansikova, H., Pecina, P., Tesarova, M., Cerna, L., Houstek, J., Zeman, J. (2005) Tissue-specific cytochrome c oxidase assembly defects due to mutations in SCO2 and SURF1. *Biochem. J.* **392**, 625-632.

Stiburek, L., Hansikova, H., Tesarova, M., Cerna, L., Zeman, J. (2006) Biogenesis of eukaryotic cytochrome c oxidase. *Physiol. Res.* **55(Suppl 2)**, S27-S41.

Stiburek, L., Vesela, K., Hansikova, H., Hulkova, H., Zeman, J. (2009) Loss of function of Sco1 and its interaction with cytochrome c oxidase. *Am. J. Physiol. Cell. Physiol.* **296,** C1218-1226.

Takahashi, Y., Kako, K., Kashiwabara, S., Takehara, A., Inada, Y., Arai, H., Nakada, K., Kodama, H., Hayashi, J., Baba, T., Munekata, E. (2002) Mammalian copper chaperone Cox17p has an essential role in activation of cytochrome c oxidase and embryonic development. *Mol. Cell Biol.* **22**, 7614-7621.